

# Pressure-induced phase transition of wulfenite<sup>\*</sup>

LIU Ying-Xin(刘迎新)<sup>1</sup> QIN Shan(秦善)<sup>1;1)</sup> WU Jing(吴婧)<sup>1</sup>

LI Xiao-Dong(李晓东)<sup>2</sup> LI Yan-Chun(李延春)<sup>2</sup> LIU Jing(刘景)<sup>2</sup>

1 (Key Laboratory of Orogenic Belts and Crustal Evolution of MOE, Department of Geology, Peking University, Beijing 100871, China)

2 (Institute of High Energy Physics, Chinese Academy of Sciences, Beijing 100049, China)

**Abstract** The in-situ high-pressure structures of wulfenite have been investigated by means of angular dispersive X-ray diffraction with diamond anvil cell and synchrotron radiation. In the pressure up to 22.9 GPa, a pressure-induced scheelite-to-fergusonite transition is observed at about 10.6 GPa. The pressure dependence for the lattice parameters of wulfenite is reported, and the axial compression coefficients  $Ka_0 = -1.36 \times 10^{-3} \text{ GPa}^{-1}$  and  $Kc_0 = -2.78 \times 10^{-3} \text{ GPa}^{-1}$  are given. The room-temperature isothermal bulk modulus is also obtained by fitting the P-V data using the Murnaghan equation of state.

**Key words** wulfenite, high-pressure, phase transition, synchrotron radiation, X-ray diffraction

**PACS** 91.60.Gf, 91.60.Fe, 91.60.Hg

## 1 Introduction

The high-pressure behaviors of hypergenic minerals are very helpful to understand the geological process relative to the lithospheric slab subduction, due to the re-distribution of fluids and elements with increasing temperature and pressure.

Wulfenite, a typical hypergenic mineral, is a scheelite-structure molybdate with space group  $I4_1/a$  and chemical formula  $\text{PbMoO}_4$ . The first high-pressure experiment on wulfenite was carried out by Ganguly and Nicol<sup>[1]</sup> in 1977 based on Raman spectra, in the pressure up to 4 GPa, they found no evidence of structural transformation but predicted that molybdates with heavier cations in scheelite-type structure would have a different high-pressure structure from wolframite. The high-pressure Raman study on scheelite-structure compounds  $\text{PbMoO}_4$  and  $\text{PbWO}_4$  was also taken by Jayaraman et al.<sup>[2]</sup>, in the higher pressure range, the pressure-induced phase transitions near 4.5 GPa for  $\text{PbWO}_4$  and near 9.5 GPa for  $\text{PbMoO}_4$  were reported. The authors gave no details for the first-order phase transitions. Using high-pressure X-ray diffraction, Hazen et al.<sup>[3]</sup> studied the high-pressure crystal chemistry of several

scheelite-type tungstates and molybdates, they found no phase transition for  $\text{PbMoO}_4$  up to 6.0 GPa, but observed a first-order phase transition for  $\text{PbWO}_4$  at about 5.0 GPa. Errandonea et al. investigated the high-pressure behavior of  $\text{PbWO}_4$  in the pressure up to 24 GPa by means of X-ray diffraction and X-ray absorption near-edge structure and found a pressure-driven transition, from the tetragonal scheelite to monoclinic fergusonite structure with space group  $C2/c$ , at 9 GPa<sup>[4]</sup>. However, Yu et al. claimed that  $\text{PbMoO}_4$  undergoes a crystal to amorphous phase transition between 9.2 and 12.5 GPa under non-hydrostatic conditions<sup>[5]</sup>. Otherwise, Nakamura et al. synthesized the scheelite group minerals and confirmed that the complete solid solutions exist in the  $\text{CaWO}_4$ - $\text{CaMoO}_4$  and  $\text{PbMoO}_4$ - $\text{PbWO}_4$  systems<sup>[6]</sup>.

In this study, we explore the pressure stability of wulfenite, by using angular dispersive X-ray diffraction (ADXRD) with diamond anvil cell (DAC) and synchrotron radiation, in a higher hydrostatic pressure range up to 22.9 GPa.

## 2 Experiments

The wulfenite sample used in this study is a

Received 18 December 2008

<sup>\*</sup> Supported by NSFC (40672024) and Knowledge Innovation Project of the Chinese Academy of Sciences (KJCX2-SW-N20, KJCX2-SW-N03)

1) Corresponding author, E-mail: sqin@pku.edu.cn

©2009 Chinese Physical Society and the Institute of High Energy Physics of the Chinese Academy of Sciences and the Institute of Modern Physics of the Chinese Academy of Sciences and IOP Publishing Ltd

saffron yellow perfect crystal with tetragonal plate shape, collected from a lead-zinc deposit in Guizhou Province, China. The in-situ high-pressure ADXD measurements were carried out in a 400  $\mu\text{m}$  culet Mao-Bell DAC, a mixture of methanol, ethanol and water with 16:4:1 ratio was used as pressure medium. The wulfenite crystal was ground to powder in an agate mortar and then loaded together with a ruby chip into a hole of 150  $\mu\text{m}$  in diameter drilled on a T301 stainless steel gasket which was pressurized to 35  $\mu\text{m}$  thick. The pressure was measured by the shift of the R1 photoluminescence line of ruby<sup>[7]</sup>.

The ADXD experiment was performed at the 4W2 High-pressure Station of the Beijing Synchrotron Radiation Facility (BSRF). A highly collimated beam with a 70  $\mu\text{m}$   $\times$  130  $\mu\text{m}$  size was focused on the sample. Monochromatic synchrotron radiation at  $\lambda = 0.620140 \text{ \AA}$  was used for data collection with  $2\theta$  ranging between  $5^\circ$  and  $25^\circ$ . Twenty runs up to 22.9 GPa were carried out and each spectrum was collected for 600 s at every pressure interval. The diffraction images collected from a MAR345 image plate were integrated and corrected for distortions using FIT2D<sup>[8]</sup> to yield intensity versus  $2\theta$  diagrams.

### 3 Results and discussion

The X-ray diffraction spectrum of  $\text{PbMoO}_4$  at

ambient conditions is almost the same as the JCPDS card 74-1075, which then was used as a standard to index the diffraction peaks. The cell parameters,  $a = 5.459 (11) \text{ \AA}$ ,  $c = 12.156 (36) \text{ \AA}$  and  $V = 362.2 (15) \text{ \AA}^3$  with space group  $I4_1/a$ , were refined with the Rietveld method using the UnitCell software<sup>[9]</sup>.

The in-situ high-pressure ADXD spectra of  $\text{PbMoO}_4$  recorded at different pressures are presented in Fig. 1, in which twelve diffraction peaks could be identified in the lower pressure range. With the increase of pressure, the Gaussian-type diffraction peaks of wulfenite shift to the higher angle. The relative intensities of 105 and 220 peaks strength gradually with increasing pressure, but for most of the diffraction lines, due to the sample thinned and the possible increasing of structural disorder, the intensity decreases and peak broadens gradually, even several weak peaks disappear. For example, the very weak peaks 132 and 224 in higher angle disappear at a very low pressure (1.5 GPa). However, the weak lines in lower angle, such as 101, 004, 200 and 211, disappear simultaneously at around 10.6 GPa, which might be resulted from the structural change. By the same reason, the doublet (123 and 204) merges into a single peak also at 10.6 GPa. The  $d$ -spacings of diffraction lines, as a function of pressure, are exhibited in Fig. 2, in which it is clearly seen that five diffraction reflections vanish at 10.6 GPa. From the

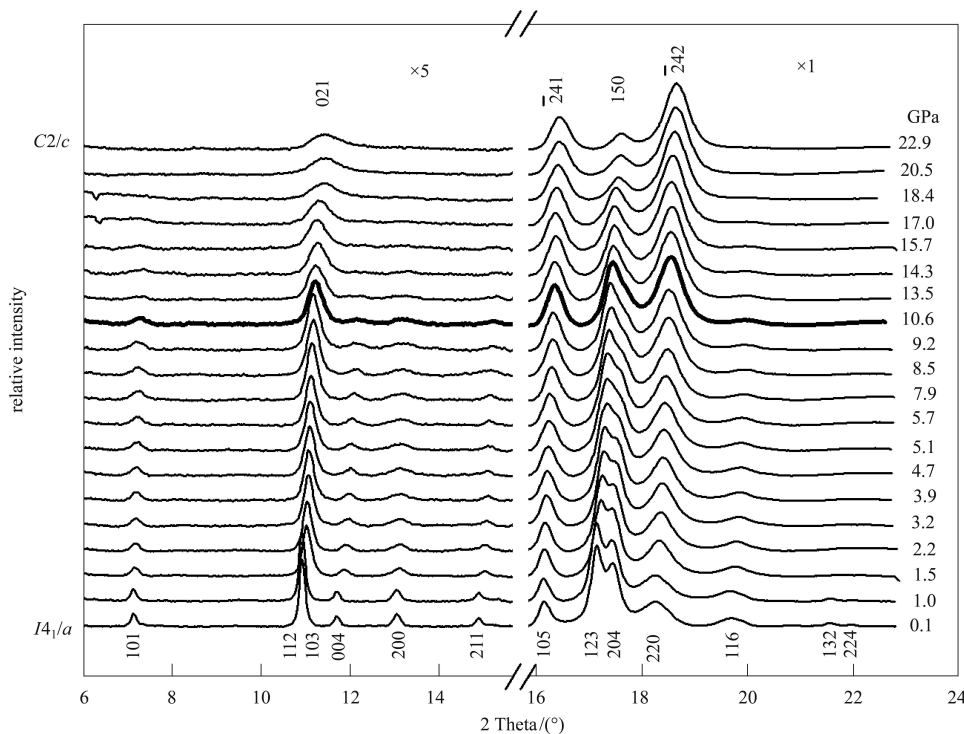


Fig. 1. ADXD patterns of wulfenite at pressures up to 22.9 GPa. The peaks in low angle region are multiplied by a factor of 5 in order to improve visibility. The spectrum marked with bold line is the phase transition boundary.

peak disappearing and merging, it is proposed that the structure of wulfenite should have a transformation at 10.6 GPa due to the pressure effect.

The phase transition boundary at 10.6 GPa observed by X-ray diffraction here is close to that obtained from the Raman result<sup>[2]</sup>, which gives the boundary at 9.5 GPa. The values of transition pres-

sure obtained from Raman scattering tend to be slightly lower than that obtained by the X-ray diffraction on the same material<sup>[10]</sup>. The same situation also occurs in the scheelite-structure tungstates, for instance the  $\text{PbWO}_4$ , its transition pressure obtained from Raman spectrum is 4.5 GPa<sup>[2]</sup>, while that from XRD is 9.0 GPa<sup>[4]</sup>.

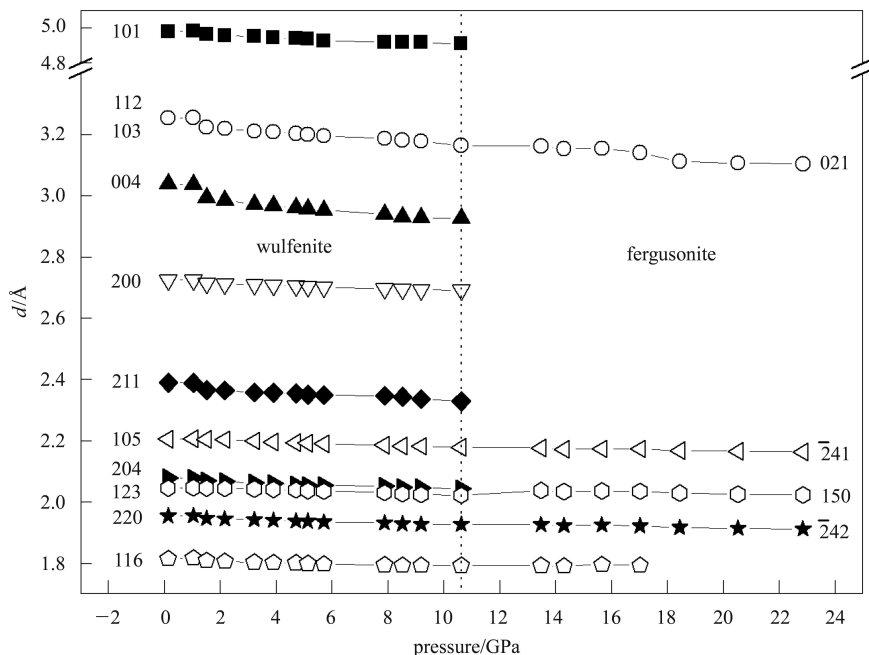


Fig. 2. Pressure dependence of the  $d$ -spacing of  $\text{PbMoO}_4$ . The dotted line shows the pressure boundary of the phase transition.

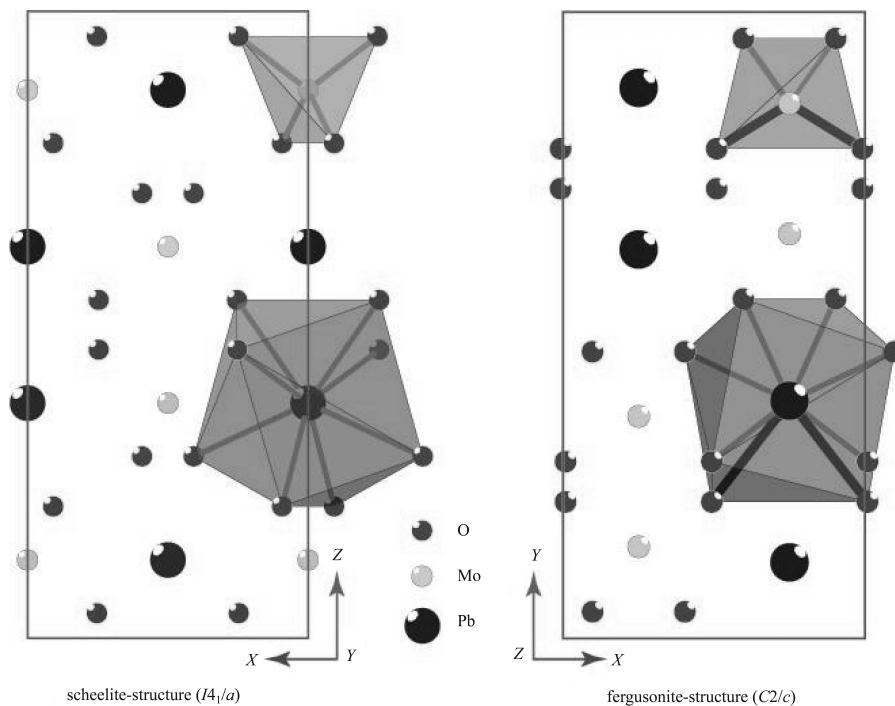


Fig. 3. The scheelite and fergusonite structures of  $\text{PbMoO}_4$ . The  $\text{PbO}_8$  and  $\text{MoO}_4$  polyhedra are illustrated, two Pb-O and Mo-O bonds (shown as dark lines) are enlarged as the consequence of the scheelite to fergusonite phase transition.

With the increasing pressure above 10.6 GPa, seen in Fig. 1 and Fig. 2, most diffraction lines disappear. Only four diffraction peaks remain when the pressure is up to 22.9 GPa, which could be indexed as 021,  $\bar{2}41$ , 150 and  $\bar{2}42$  respectively with the fergusonite structure. The peak positions and relative intensities are consistent with those in the JCPDS card 72-2077. That means  $\text{PbMoO}_4$  would transfer from tetragonal  $I4_1/a$  to monoclinic  $C2/c$  under pressure. The sequence of phase transition of  $\text{PbMoO}_4$  is the same as that of  $\text{PbWO}_4$ <sup>[3, 4]</sup>. Although Yu et al. reported the amorphous transformation for the same material between 9.2 and 12.5 GPa, that may be caused by the lack of pressure-transmitting medium because of a nonhydrostatic pressure environment. According to Errandonea<sup>[11]</sup>, the scheelite-to-fergusonite transition is caused by the slightly distorted  $\text{MoO}_4$  tetrahedra and quite distorted  $\text{PbO}_8$  polyhedra. During the pressure increase, the volume of  $\text{MoO}_4$  tetrahedra is enlarged and that of  $\text{PbO}_8$  polyhedra decreased in  $\text{PbMoO}_4$  scheelite-structure, which are the consequences of a slight decrease of two Mo-O bonds and the increase of the other two Mo-O bonds inside the  $\text{MoO}_4$  tetrahedra, and six of the Pb-O bonds in the  $\text{PbO}_8$  polyhedra compressed and the remaining two enormously expanded (Fig. 3).

The pressure dependence of the lattice parameters for  $\text{PbMoO}_4$  up to 10.6 GPa is shown in Fig. 4, both of the cell lengths and volume show a smooth decrease with increasing pressure. Fig. 4(a) plots the axial compressibilities, it is clearly seen that the  $c$  axis is more compressible than  $a$  axis. By a linear fitting, the axial compression coefficients were obtained as  $Ka_0 = -1.36 \times 10^{-3} \text{ GPa}^{-1}$  and  $Kc_0 = -2.78 \times 10^{-3} \text{ GPa}^{-1}$ . The  $Ka_0/Kc_0$  ratio is 0.49. This phenomenon can be

related to the fact that when pressure is applied to the scheelite-structure  $\text{PbMoO}_4$ , the  $\text{MoO}_4$  tetrahedra remain essentially undistorted while the volume of the  $\text{PbO}_8$  is largely reduced<sup>[3]</sup>. Therefore,  $a$  axis is expected to be less compressible than  $c$  axis because the  $\text{MoO}_4$  units are directly aligned along the  $a$  axis whereas there is an Pb cation between the  $\text{MoO}_4$  tetrahedra along the  $c$  axis<sup>[4]</sup>.

The variation of the unit-cell volume with pressure was fitted to the second-order Murnaghan equation of state (EOS), shown in Fig. 4(b). The bulk modulus ( $B_0$ ), its pressure derivative ( $B_0'$ ) and the equilibrium volume at zero pressure ( $V_0$ ) are summarized and compared with those of other scheelite-like tungstates and molybdates in Table 1. The  $V_0$  is in agreement with those of the volume we obtained above. The other two values are a little larger than the previously reported data<sup>[3, 4, 11, 12]</sup>, but still in the 70–100 GPa region predicted by the linear relationship between the bulk modulus and the value of the cation charge density<sup>[3, 11]</sup>.

Table 1. Bulk modulus ( $B_0$ ), the first pressure derivative of the bulk modulus ( $B_0'$ ), and equilibrium volume ( $V_0$ ) for scheelite tungstates and molybdates.

compound	$V_0/\text{\AA}^3$	$B_0/\text{GPa}$	$B_0'$	references
$\text{PbMoO}_4$	362.5 (6)	71(10)	29(3)	This work
$\text{PbMoO}_4$	–	64(2)	8(3)	[3]
$\text{CaWO}_4$	312 (1)	74(7)	5.6(9)	[10]
$\text{SrWO}_4$	347.4(9)	63(7)	5.2(9)	[10]
$\text{PbWO}_4$	357.8(6)	66(5)	5.6(1)	[12]
$\text{PbWO}_4$	–	64(2)	23(2)	[3]
$\text{CaWO}_4$	–	68(9)	10(1)	[3]
$\text{CaMoO}_4$	–	81.5(7)	2(1)	[3]
$\text{EuWO}_4$	348.9(8)	65(6)	4.6(9)	[4]

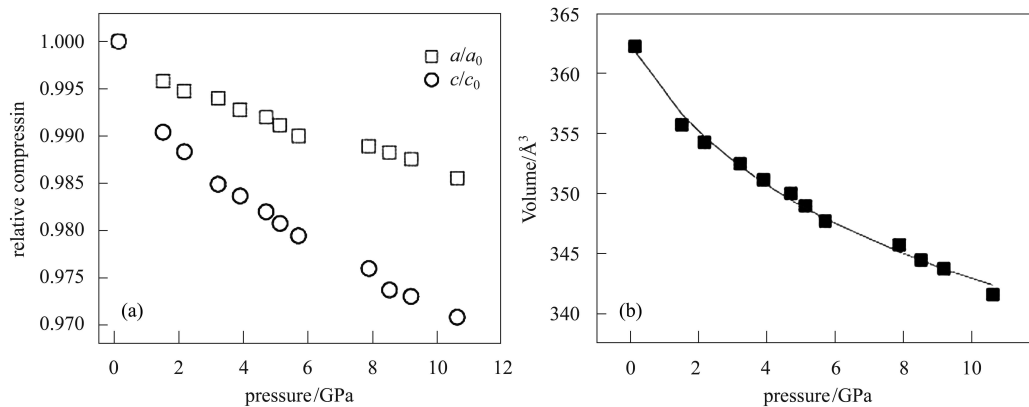


Fig. 4. Relative compression of wulfenite. The evolution of relative axial ratio (a) and the variation of volume (b) as a function of pressure are shown. The solid line in (b) represents the Murnaghan EOS fitted to the P-V data.

## 4 Conclusions

The in-situ high-pressure structures of hypergenic mineral wulfenite have been investigated using ADXD and DAC technics under pressure up to 22.9 GPa. The results confirm the existence of a scheelite-to-fergusonite phase transition of  $\text{PbMoO}_4$  under hydrostatic condition. The boundary of phase transition is located at about 10.6 GPa. This

pressure-induced phase transition is supposed to be the consequence of the different high-pressure behaviors of polyhedra  $\text{MoO}_4$  and  $\text{PbO}_8$ . By a linear fitting, the axial compression coefficients of wulfenite are obtained as  $K_{a_0} = -1.36 \times 10^{-3} \text{ GPa}^{-1}$  and  $K_{c_0} = -2.78 \times 10^{-3} \text{ GPa}^{-1}$ . The pressure dependence of cell volume of wulfenite is fitted to the Murnaghan EOS, yielding a room-temperature isothermal bulk modulus 71(10) GPa.

---

## References

- 1 Ganguly B N, Nicol M. *Physica Status Solidi B*, 1977, **79**(2): 617
- 2 Jayaraman A, Batlogg B, VanUitert L G. *Physical Review B*, 1985, **31**(8): 5423
- 3 Hazen R M, Finger L W, Mariathasan J W E. *Journal of Physics and Chemistry of Solids*, 1985, **46**(2): 253
- 4 Errandonea D, Pellicer-Porres J, Manjón F J et al. *Physical Review B*, 2006, **73**: 224103
- 5 YU Cui-Ling, YU Qing-Jiang, GAO Chun-Xiao et al. *Chinese Physics Letters*, 2007, **24**(8): 2204
- 6 Nakamura T, Sugiyama K, Moriguchi E et al. Shigen-to-Sozai, 2002, **118**: 217
- 7 Barnett J D, Block S, Piermari G J. *Review of Scientific Instrument*, 1973, **44**: 1
- 8 Hammersley A P, Svensson S O, Hanfland M et al. *High Pressure Research*, 1996, **14**: 235
- 9 Holland T J B, Redfern S A T. *Mineralogical Magazine*, 1997, **61**: 65
- 10 Besson J M, Itie J P, Polian A et al. *Physical Review B*, 1991, **44**: 4214
- 11 Errandonea D, Pellicer-Porres J, Manjón F J et al. *Physical Review B*, 2005, **72**: 174106
- 12 Errandonea D. *Physica Status Solidi B*, 2005, **242**(14): R125